MATERIALS AND INTERFACES

Development of Porosity upon Chemical Activation of Kraft Lignin with $ZnCl_2$

E. Gonzalez-Serrano, T. Cordero, J. Rodríguez-Mirasol, and J. J. Rodríguez*

Department of Chemical Engineering, University of Málaga, 29071 Málaga, Spain

Chemical activation of kraft lignin with $ZnCl_2$ allows one to obtain high surface area activated carbons with a predominantly microporous structure. Most of porosity develops within the thermal range of 400−500 °C, where an increase of temperature leads to increasing micropore volume values (up to ≈1 cm^3/g) and a wider distribution of micropore size. An increasing mesoporositiy is also observed. Increasing the impregnation ratio ($ZnCl_2$/lignin, wt) has a similar effect on the evolution of the porous structure. The mesopore distribution remains within the low-size range even at high impregnation ratios (up to 2.3). At 500 °C and an impregnation ratio of 2.3, where the highest contribution of mesoporosity was observed, the mesopore volume reached a value of 0.59 cm^3/g. These conditions allowed us to obtain a BET surface area of 1800 m^2/g, including the external or non-microporous surface of 200 m^2/g. The porous structure developed suggests a fairly homogeneous distribution of the activating agent favored by the softening and partial fusion which kraft lignin undergoes within the temperature range of 180−280 °C.

Introduction

Kraft lignin is a modified form of lignin which can be isolated by acid precipitation from the black liquors of kraft pulp mills. These black liquors are commonly processed through evaporation and calcination to recover energy and the remaining chemical reactant. Nevertheless, lignin has gained within the last two decades an increasing interest as a potential raw material for the chemical industry. Among other uses, lignin, as a carbonaceous material, can be viewed as a potential precursor for activated carbons.

In previous works we have reported our results on "physical" activation of eucalyptus kraft lignin by CO_2 partial gasification (Rodríguez-Mirasol et al., 1993a,b). In this paper we study "chemical" activation of this precursor using $ZnCl_2$ as the activating agent.

The scientific literature contains some interesting papers on $ZnCl_2$ activation of different lignocellulosic wastes like almond shells (Ruiz-Beviá et al., 1984a,b; Torregrosa and Martín-Martínez, 1991), peach stones (Caturla et al., 1991), olive stones (Rodríguez-Reinoso and Molina-Sabio, 1992) and holm oak sawdust (Blasco et al., 1989).

Experimental Section

The raw material used in this work was kraft lignin from Eucalyptus Grandis which has been conveniently characterized elsewhere (Rodríguez-Mirasol et al., 1993a,b). The lignin as supplied had a 12.4% ash content which was reduced up to 0.1% by washing with 1 wt % H_2SO_4 aqueous solution followed by distilled water at 60 °C. Once washed, the lignin was impregnated with the activating agent $ZnCl_2$. The impregnation was carried out in a rotary evaporator using 100 mL of $ZnCl_2$ aqueous solution. The $ZnCl_2$ concentration and the weight of lignin were adjusted in each experiment to obtain the required $ZnCl_2$/lignin weight ratio, namely the impregnation ratio. This was varied within the range of 0.4−2.3. The mixture was held in contact in the rotary evaporator for 1 h at 30 °C and then was vacuum-evaporated. The resulting samples were stored in a vacuum dryer at 60 °C and 0.05 atm.

Activation was carried out through thermal treatment of the impregnated samples in an inert atmosphere. This pyrolysis or carbonization process was performed in a conventional horizontal furnace consisting of a 120 cm length and 7 cm i.d. silica-glass tube heated by electrical resistance at a controlled temperature. Sample weights in the vicinity of 8 g were always used, and certified 99.998% N_2 was continuously passed at a 200 mL (STP)/min flow rate. Different activation temperatures within the 350−600 °C range were investigated. In each run the activation temperature was reached at a 10 °C/min heating rate and then maintained for 1 h. The system was then cooled down while maintaining the N_2 flow. The resulting carbons were washed in successive batches with aqueous HCl solution until no Zn^{2+} was detected by AA in the filtrate and then with distilled water until negative Cl^- analysis. The liquid resulting from the washing stages with HCl solution was analyzed for Zn^{2+} by AA to determine the recovery percentage in each experiment.

Previous to the activation runs we carried out some thermogravimetric (TG) experiments in an N_2 atmosphere to learn about the thermal decomposition of the $ZnCl_2$-impregnated kraft lignin. A CI Electronics thermogravimetric system described elsewhere (Rodríguez-Mirasol et al., 1993c) was used. A sample weight in the vicinity of 10 mg and a 10 °C/min heating rate were used.

The porous structure of the resulting activated carbons was characterized from 77 K N_2 adsorption−

* Author to whom correspondence should be addressed. Phone: 34-5-2131916. Fax: 34-5-2132000. E-mail: jjrj@uma.es.

S0888-5885(97)00261-3 CCC: $14.00

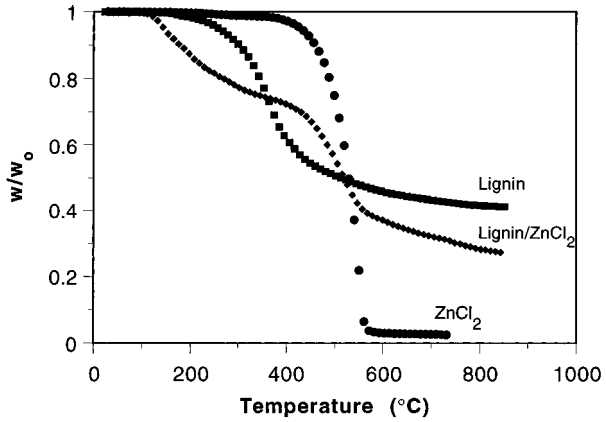

Figure 1. TG curves for thermal decomposition of $ZnCl_2$-impregnated kraft lignin, pure kraft lignin, and $ZnCl_2$.

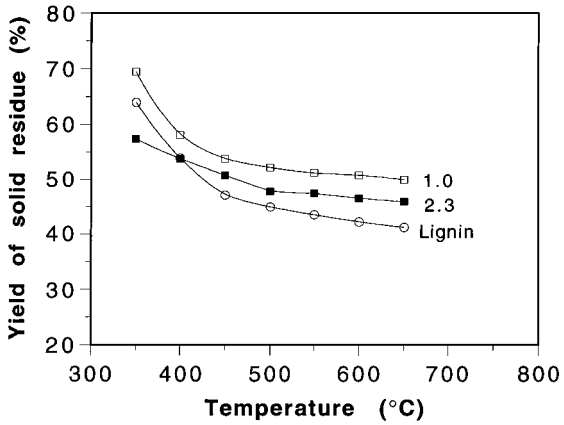

Figure 2. Carbonization yields (solid residue) as a function of temperature of $ZnCl_2$-impregnated kraft lignin (impregnation ratios 1 and 2.3) and pure kraft lignin.

desorption, 273 K CO_2 adsorption, and mercury porosimetry (MP). This last was carried out in a Carlo Erba porosimeter 4000. The N_2 and CO_2 adsorption isotherms were obtained in an Autosorb-1. The samples were previously outgassed at 523 K for 12 h to a residual pressure of about 10^{-5} Torr.

To learn about the microporosity of the activated carbons, we have obtained different micropore volumes by applying the Dubinin−Radushkevich (DR) equation (Dubinin, 1966) to the CO_2 and N_2 adsorption data and the α_s method (Sing, 1970) to the N_2 adsorption values. Also, we have obtained the micropore size distribution from the MP method (Mikhail et al., 1968) applied to the N_2 adsorption isotherms. From the N_2 and CO_2 isotherms we have obtained the BET and the DR surface areas, respectively, using 0.162 nm^2 as the cross-sectional area of the N_2 molecule (Gregg and Sing, 1982) and 0.187 nm^2 for CO_2 (Rodríguez-Reinoso, 1986). The α_s method allows one also to obtain the values of the so-called external surface, namely the surface area associated to the non-microporous structure (Sing, 1970). The macropore volume and size distribution were derived from the mercury intrusion curves, whereas with regard to mesopore volume the information obtained from mercury porosimetry needs to be complemented in order to cover the pore range between 2 and 4 nm diameter. In this work, the mesopore volume corresponding to that range was derived from the N_2 adsorbed volume up to the relative pressure which corresponds to a pore diameter of 4 nm according to the Kelvin equation, discounting the micropore volume derived from the α_s method. The mesopore size distribution was obtained from the Barret, Joiner, and Halenda method (1951).

Results and Discussion

TG Study of Thermal Decomposition of $ZnCl_2$-Impregnated Kraft Lignin. Figure 1 shows the weight-loss curve of $ZnCl_2$-impregnated kraft lignin with an impregnation ratio of 1 in N_2 atmosphere and at a 10 °C/min heating rate. For the sake of comparison we have included the corresponding curves for pure kraft lignin and $ZnCl_2$. As can be seen, the presence of $ZnCl_2$ has a significant effect on the thermal decomposition of kraft lignin. Devolatilization starts well bellow 200 °C and proceeds up to about 400 °C. The second stage of the weight-loss curve can be essentially attributed to volatilization of $ZnCl_2$ itself. At 900 °C kraft lignin yields 40% of carbon residue which is lower than that obtained for the $ZnCl_2$-impregnated sample if we assume a complete volatilization of $ZnCl_2$ at that temperature (≈49%).

Development of Porosity upon Activation. We have considered the effect of two main variables on the activation process with regard to the development of the porous structure: The impregnation ratio (as defined in the Experimental Section) and the heat treatment temperature. Five different impregnation ratios have been checked within the range 0.4−2.3. At each impregnation ratio different activated carbons were prepared at temperatures ranging from 350 to 600 °C.

Figure 2 shows the yield values (weight of washed activated carbon relative to that of the starting kraft lignin, both in dry basis) obtained in the experiments performed in the activation furnace. For the sake of comparison we have included also the yield values corresponding to the carbonization of kraft lignin itself at the same temperatures and soaking time. These values confirm that the pyrolytic decomposition giving rise to volatile matter loss takes place mainly within the thermal range extending up to 400 °C and above that temperature the yield values approach to a practically constant level which is somewhat dependent on the impregnation ratio. A similar trend has been encountered in other works using almond shells (Ruiz-Beviá et al., 1984a,b) and holm oak wood (Blasco et al., 1989) as starting materials. In the absence of chemical agents kraft lignin produces a significantly higher carbonization yield than lignocellulosic precursors. The use of $ZnCl_2$ increases the carbonization yield, but the quantitative effect is markedly less important for lignin in comparison with lignocellulosics.

Effect of the Activation Temperature. Figure 3 shows the 77 K N_2 adsorption−desorption isotherms of activated carbons obtained at different temperatures using an impregnation ratio of 1. As a primary general observation the total adsorbed volume, which provides a first approximation of porosity development, increases with increasing activation temperature up to 500 °C and then decreases significantly at 600 °C. This general observation can be analyzed in the context of the corresponding yield values of Figure 2. Up to about 400 °C the development of porosity can be explained quite consistently as the result of volatile matter loss. Above that temperature the yield decreases quite smoothly whereas a significant development of porosity still takes place up to 500 °C. Thus, the evolution of porosity within the thermal range of 400−500 °C cannot be

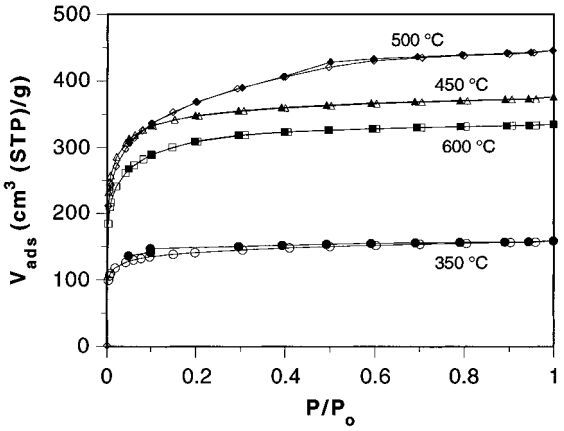

Figure 3. N_2 adsorption−desorption isotherms (77 K) of activated carbons obtained at different temperatures with an impregnation ratio of 1. (Open symbols, adsorption. Closed symbols, desorption.)

attributed solely to weight loss but in a great part to a reorganization of the carbon structure. At 600 °C the porosity of the activated carbons undergoes a significant decrease which can be due to a contraction of the pore structure as a result of heat treatment. A similar shift in porosity development with activation temperature has been reported by Caturla et al. (1991) for $ZnCl_2$ activation of peach stones.

The isotherms of Figure 3 belong to the type I of the BDDT classification (Brunauer et al., 1940), indicative of an essentially microporous structure. Nevertheless, the evolution of the shape of the isotherms reveals some significant differences in porosity distribution with activation temperature which deserve a more detailed analysis.

At low temperature (350 °C) the isotherm exhibits an almost horizontal plateau starting at very low relative pressure. This indicates that the porous structure consists very predominantly of narrow micropores, namely pores whose width is around 1−2 times the smaller dimension of the adsorptive molecule (0.3 nm) and whose filling occurs at very low relative pressure (high potential values) due to enhancement of the adsorption energy. The desorption branch does not meet the adsorption curve even at relative pressures as low as 0.1, thus indicating that the adsorption values obtained at low relative pressures must not correspond to equilibrium. This problem persisted even when increasing substantially the equilibration time, confirming the narrow microporous structure of the activated carbon where the N_2 molecules are subjected to severe diffusional limitations.

Increasing the activation temperature leads to a substantial increase of micropore volume, as revealed by the adsorption values at low relative pressures, but it is also important that the isotherms exhibit a more open knee which extends up to increasingly higher relative pressures as activation temperature increases up to 500 °C. These features indicate a progressive widening of the microporosity.

The plateau-like region of the isotherms shows a higher slope with increasing activation temperature within the aforementioned range. This is indicative of a higher contribution of mesoporosity. At 500 °C the existence of a hysteresis loop of H4 type is clearly noticeable (Sing et al., 1985), associated to type I isotherms, which closes at 0.4 relative pressure, indicative of capillary condensation in mesopores. This trend in the evolution of the porous structure with activation

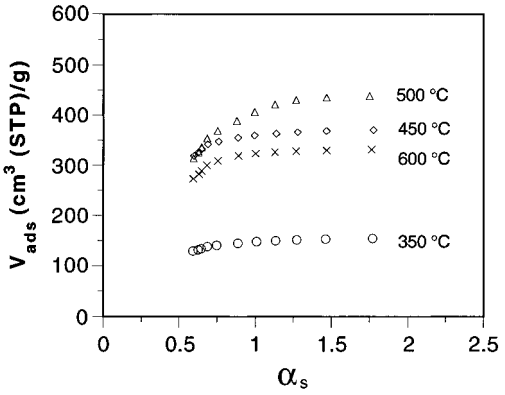

Figure 4. α_s plots of activated carbons obtained at different temperatures (impregnation ratio = 1).

temperature undergoes a shift somewhere between 500 and 600 °C, and at this last temperature the isotherm reveals a lower and narrower porosity.

Figure 4 provides useful information with regard to the above discussion. It presents the α_s plots derived from the isotherms of Figure 3. In these plots, the amount of N_2 adsorbed is represented versus α_s, namely the ratio of the amount adsorbed by a nonporous standard at each relative pressure and at $P/P_0 = 0.4$. In this work we have used as the standard Elftex-120, an ungraphitized carbon black (Carrott et al., 1987a). The linear region of these plots corresponds to adsorption on the non-microporous surface of the solid. Back-extrapolation of that linear branch provides the value of total micropore volume (in this case, after converting the gas adsorbed volume to liquid N_2 volume). The values are reported in Table 1 and confirm the development of microporosity upon activation as the temperature increases up to 500 °C. A further decrease of micropore volume takes place at 600 °C. This can be explained as the result of a contraction of the structure upon thermal treatment which reduces the amount of pores accessible to N_2 or can be also attributed to a higher loss of $ZnCl_2$ through volatilization, thus reducing the activating agent-to-lignin weight ratio.

From the α_s plots one can also obtain information about the distribution of micropore size. First, it can be noticed that the downward deviation of the α_s plot starts at higher α_s values as activation temperatures increase up to 500 °C. This is indicative of a broadening of microporosity (Carrot et al., 1987b; Rodríguez-Reinoso et al., 1989). On the other hand the back-extrapolation of the downward deviation branch of the α_s plots provides a semiquantitative approach of the relative contribution of narrow micropores (where adsorption takes place through a primary filling mechanism, occurring at relative pressure up to about 0.01) and larger micropores, namely those filled by a secondary or cooperative mechanism at higher relative pressures (up to about 0.2−0.3) (Carrot et al., 1987b). The lower the intercept of the aforementioned back-extrapolation with respect to the total micropore volume, the lower the contribution of narrow micropores to the total microporosity (Carrott and Sing, 1988). This effect can be noticed in our case and confirms again the widening of the micropore size distribution of the activated carbons as the activation temperature increases up to 500 °C.

To obtain better knowledge of the microporosity of these activated carbons, we obtained the 273 K CO_2 adsorption isotherms up to 1 atm pressure (≈0.03 relative pressure). The Dubinin−Raduskhevich (DR) equation applied to these adsorption values allows one

Table 1. Micropore Volumes of Activated Carbons Obtained at Different Temperatures (Impregnation Ratio = 1)

temperature (°C)	micropore volumes (cm^3/g)		
	V_s (N_2, 77 K)	DR (N_2, 77 K)	DR (CO_2, 273 K)
350	0.211	0.217	0.224
400	0.515	0.520	0.343
450	0.528	0.511	0.396
500	0.634	0.545	0.406
600	0.476	0.453	0.321

to obtain the corresponding micropore volume, whose values are reported in Table 1, together with the DR micropore volume values derived from the 77 K N_2 isotherms and those obtained from the above-discussed α_s method. The comparison of these values clearly confirms our previous conclusions. At low activation temperature (350 °C) the micropore volume obtained with CO_2 is higher than the corresponding α_s volume. This indicates that at low temperature basically only narrow microporosity develops. As indicated above the CO_2 isotherms cover the relative pressure range up to 0.03. At these low relative pressure values only narrow micropores are filled. Although the α_s method applied to the N_2 isotherms accounts for the complete microporosity, diffusional limitations of N_2 at 77 K in narrow micropores avoid reaching the adsorption capacity corresponding to equilibrium, giving rise to a lower volume than that obtained with CO_2 at 273 K.

At higher activation temperatures the α_s micropore volumes always become significantly higher than the CO_2 ones, thus confirming the appreciable widening of microporosity which accompanies an increase of activation temperature. This difference reaches its higher value at 500 °C and then decreases again. Nevertheless, even at that temperature the relative contribution of narrow micropores is still fairly important, representing almost a 65% of the total micropore volume. On the other hand, the values of the micropore volume obtained with N_2 from the DR equation and from the α_s method become quite similar except for the 500 °C activated carbon. This suggests that the relative contribution of larger micropores must be small except for that carbon. Thus, to obtain a well-developed microporosity, a temperature around 500 °C is recommended.

The porous structure of these activated carbons consisting predominantly of small micropores suggests a quite homogeneous distribution of the activating agent within the solid structure of the precursor. This is likely unattainable during the impregnation process due to the nonporous character of that kraft lignin and seems most probable to occur upon heating during the activation stage. To investigate this point, we performed some experiments where $ZnCl_2$-impregnated kraft lignin with different impregnation ratios was heated in glass flasks under continuous N_2 flow. Upon heating, a softening or partial fusion was observed, starting somewhere between 180 and 200 °C and extending up to 250−280 °C (these temperatures depending somehow on the impregnation ratio) where resolidification occurs. The occurence of this partial fusion stage facilitates diffusion of $ZnCl_2$, giving rise to a fairly homogeneous distribution.

The slope of the linear region of the α_s plots allows one to calculate the external or non-microporous surface area of the activated carbons (Sing, 1970). The corresponding values are shown in Table 2 which includes also the BET surface area. With regard to this, it can be seen that the values obtained compare fairly well

Table 2. BET and External Surface Areas of Activated Carbons Obtained at Different Temperatures (Impregnation Ratio = 1)

temperature (°C)	A_{BET} (m^2/g)	A_s (m^2/g)
350	534	30
400	1297	75
450	1320	86
500	1347	111
600	1153	70

Table 3. Meso- and Macropore Volume of Activated Carbons Obtained at Different Temperatures (Impregnation Ratio = 1)

temperature (°C)	$V_{mesopore}$ (cm^3/g)	$V_{macropore}$ (cm^3/g)
350	0.031	0.119
400	0.096	0.109
450	0.131	0.302
500	0.151	0.148
600	0.023	0.202

with those of good-quality commercial activated carbons. The external surface area shows higher values with increasing activation temperature, again up to 500 °C, thus indicating an increasing contribution of mesoporosity. Nevertheless, the external surface area shows always moderate values, indicating that these carbons obtained through chemical activation of kraft lignin with $ZnCl_2$ are essentially microporous solids.

The values of meso- and macropore volumes are reported in Table 3. When comparing these results with those obtained by some other authors from different precursors, our activated carbons show higher meso- and macropore volumes than those reported by Torregrosa et al (1991) who worked with almond shells at the same impregnation ratio whereas Kadlec et al (1970) encountered a higher development of mesoporosity and lower development of macroporosity when studying a $ZnCl_2$ activated carbon obtained from coconut shell. Looking at the evolution of the macropore volume values, one cannot establish a systematic dependence of macroporosity development with the activation temperature. All the activated carbons exhibit lower macropore volumes than the starting kraft lignin (0.3 cm^3/g). As indicated before, impregnated kraft lignin undergoes a softening and partial fusion stage upon heating at relatively low temperatures. This must lead to a reorganization of the structure with a loosening of the initial macroporosity.

With regard to the distribution of mesopore size, Figure 5 reports the results obtained from the Barret, Joiner, and Halenda method showing that these activated carbons present a fairly narrow mesoporosity which mostly falls within the low mesopore range (up to about 5 nm diameter).

Effect of the Impregnation Ratio. Five different values of impregnation ratio (0.4, 0.7, 1, 1.5, and 2.3) have been checked. At each we prepared different activated carbons at temperatures ranging from 350 to 600 °C. As a representative selection Figure 6 shows the 77 K adsorption−desorption isotherms of the activated carbons obtained at 450 and 500 °C.

Both series show a common trend observed also at the remaining temperatures investigated: An increasing development of porosity accompanies the increase of the relative amount of activating agent. At all the impregnation ratios investigated the influence of the activation temperature showed the same pattern that has been discussed before, i.e., an increasing development of porosity and a widening of the porous structure as the activation temperature increases up to 500 °C.

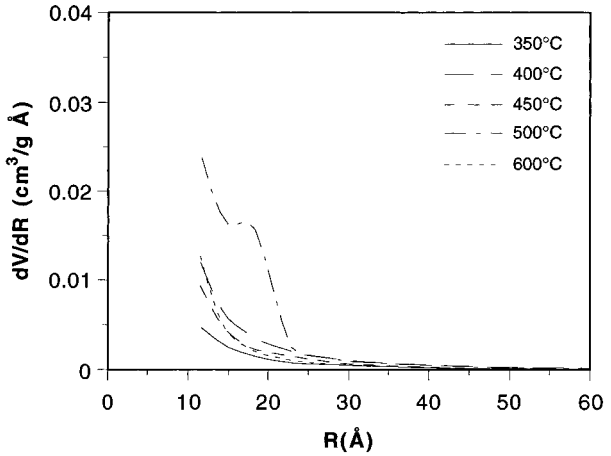

Figure 5. Mesopore size distribution of activated carbons obtained at different temperatures (impregnation ratio = 1).

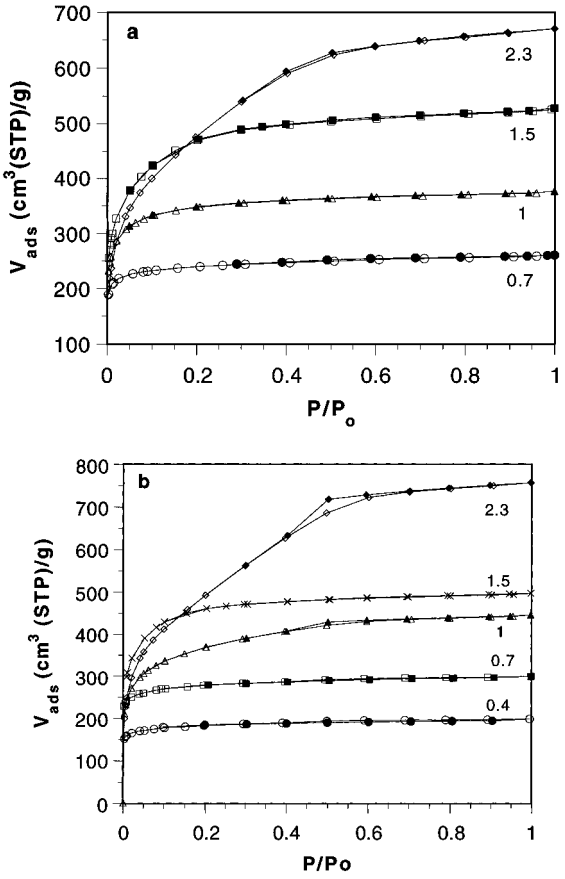

Figure 6. N_2 adsorption−desorption isotherms (77 K) of activated carbons obtained at different impregnation ratios. Activation temperatures of 450 (a) and 500 °C (b). (Open symbols, adsorption. Closed symbols, desorption.)

All the activated carbons obtained showed type I isotherms, but their shape reveals an increasingly wider porous structure as the impregnation ratio increases. Particularly at the highest impregnation ratio investigated (2.3) and at the temperatures showed in Figure 6, the isotherms clearly indicate a significant widening of the microporosity and an important development of mesoporosity. Figure 7 presents the evolution of the micropore size distribution of the activated carbons obtained at 500 °C, showing the aforementioned widening effect. At the highest impregnation ratio and a temperature of 500 °C, the micropore volume derived from the α_s method reaches a value of 1.05 cm^3/g versus 0.27 cm^3/g for the DR micropore volume obtained with

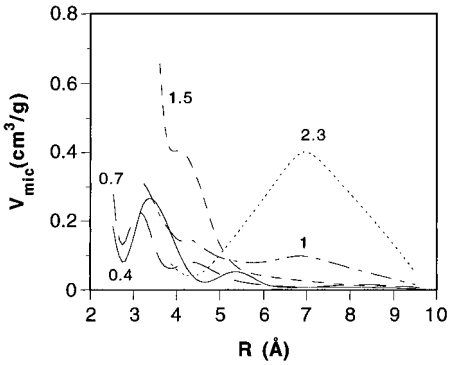

Figure 7. Micropore size distribution of activated carbons obtained at different impregnation ratios.

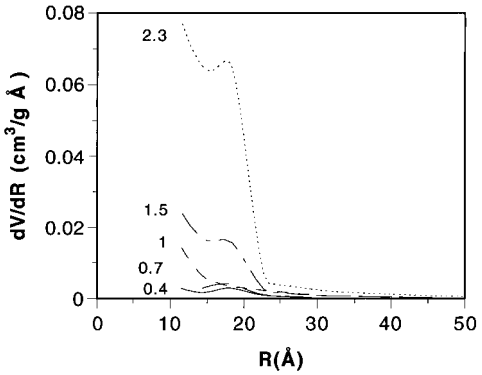

Figure 8. Mesopore size distribution of activated carbons obtained at different impregnation ratios.

Table 4. Pore Volumes of Activated Carbons Obtained at Different Impregnation Ratios

impregnation ratio	$V_{micropore}$ (cm^3/g)	$V_{mesopore}$ (cm^3/g)	$V_{macropore}$ (cm^3/g)
	temperature = 400 °C		
0.4	0.099	0.008	0.018
0.7	0.347	0.027	0.120
1.0	0.526	0.096	0.109
1.5	0.629	0.257	0.008
2.3	0.767	0.219	0.059
	temperature = 450 °C		
0.7	0.350	0.035	0.149
1.0	0.528	0.131	0.302
1.5	0.679	0.228	0.113
2.3	0.952	0.446	0.064
	temperature = 500 °C		
0.4	0.278	0.014	0.076
0.7	0.426	0.060	0.104
1.0	0.634	0.151	0.148
1.5	0.712	0.271	0.110
2.3	1.039	0.586	0.143

CO_2, this considerable difference indicating a fairly wide distribution of the microporous structure.

With regard to mesoporosity, the activated carbons obtained at the highest impregnation ratio investigated yielded mesopore volumes of 0.59 and 0.45 cm^3/g, at 500 and 450 °C activation temperature, respectively. These values are substantially higher than those previously reported at an impregnation ratio of 1 (Table 3). Nevertheless, as can be seen from the distribution curves of Figure 8, the mesopore size remains essentially within the low mesopore range (lower than 5 nm diameter).

A summary of the evolution of the porous structure of these activated carbons, varying the impregnation ratio, is presented in Table 4. As can be seen, the contribution of macroporosity stays within fairly modest values even at high impregnation ratios where one

Table 5. Recovery Percentage of Zinc (as Zn^{2+})

	impregnation ratio		
temperature (°C)	0.7	1.0	1.5
400	87	71	58
450	68	63	50
500	54	41	33
600	46	20	23

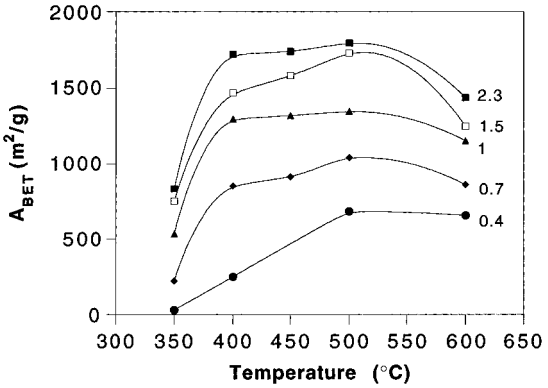

Figure 9. Evolution of the BET surface area of the activated carbons with the impregnation ratio.

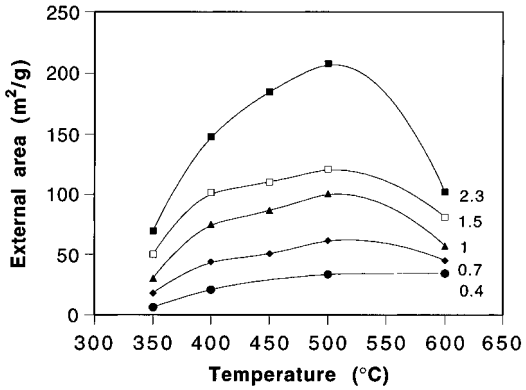

Figure 10. External surface area of the activated carbons.

would expect that the excess of activating agent should lead to an important creation of macropores through externally located devolatilization unless $ZnCl_2$ were incorporated and homogeneously distributed through the solid matrix of the precursor. Thus, the porous structure of these activated carbons, consisting essentially of micropores and small mesopores in a substantially lower extent even when high relative amounts of $ZnCl_2$ are used, supports the previously discussed conclusion of a homogeneous distribution of the activating agent favored by the softening and partial fusion which the impregnated kraft lignin undergoes at relatively low temperatures.

The evolution of the BET surface area of all the series is shown in Figure 9. As can be seen, increasing the impregnation ratio within the range investigated produces a higher development of apparent surface area. The influence of the temperature shows in all the series the trend which has already been discussed with the highest surface area values being obtained at 500 °C. At this temperature and at the highest impregnation ratio investigated (2.3), a BET surface area very close to 1800 m^2/g was reached, which compares quite favorably with that of high-quality commercial activated carbons.

With regard to the contribution of the non-microporous structure to the surface area, Figure 10 presents the evolution of the external surface area as obtained from the slope of the linear multilayer region of the α_s plots. As can be seen, impregnation ratios higher than 1 need to be used in order to attain a susbtantial development of non-microporous area. At the highest impregnation ratio investigated (2.3), a value around 200 m^2/g can be reached, which still remains well below that obtained through "physical" activation with CO_2 (Rodríguez-Mirasol et al., 1993b).

Recovery of the Activating Agent. Table 4 shows the values of percentage recovery of the activating agent as determined from the amount of zinc analyzed in the liquors resulting from activated carbons washing. As can be seen, the recovery of zinc diminishes with increasing activation temperature as a result of a higher $ZnCl_2$ evaporation. At a given activation temperature the higher the impregnation ratio the lower the percentage of Zn^{2+} recovered in the lixiviate. As the initial Zn^{2+} is balanced with the evaporated $ZnCl_2$, a low percentage of Zn^{2+} in the liquors means recovering higher amounts of $ZnCl_2$ from off gases using appropriate cleaning systems is needed. In spite of the fact that in these Zn^{2+} recovery experiments we have used a final washing stage with concentrated HCl solution (5 M), some small quantities of Zn^{2+} could still remain in the carbon matrix strongly associated to it. To check this hypothesis, we have performed X-ray and EDAX analyses in some activated carbons once the washing process has been completed. No evidence of Zn^{2+} was found in these analyses.

Conclusions and Recommendations

"Chemical" activation of kraft lignin with $ZnCl_2$ allows one to obtain activated carbons with a high BET surface area which can reach up to 1800 m^2/g. These activated carbons are essentially microporous. An increase of the activation temperature up to 500 °C and of the relative amount of activating agent within the range investigated (up to 2.3) leads to an increasingly developed porosity with a widening of microporosity and an increasing contribution of mesoporosity. The mesopore size distribution remains essentially within the low mesopore range (below about 5 nm diameter) even at high impregnation ratios.

To obtain activated carbons with a porous structure consisting essentially of narrow microporosity, which can be useful in many gas-phase adsorption applications, a moderate temperature (≈400 °C) and impregnation ratio (<1) can be used. For liquid-phase applications where a wider microporosity and a better-developed mesoporosity are in general required, a temperature in the 450−500 °C range and impregnation ratios above 1.5 are recommended.

The porous structure developed upon $ZnCl_2$ activation of kraft lignin even at high impregnation ratios suggests a fairly homogeneous distribution of the activating agent. The softening or partial fusion which kraft lignin undergoes at relatively low temperature (≈180−280 °C) may favor $ZnCl_2$ diffusion throughout the matrix of the precursor. Also, when resolidification takes place, at temperatures above the melting point of $ZnCl_2$, a microporous structure has already developed through devolatilation, allowing melt $ZnCl_2$ to migrate through this microporous net.

The plastic phase which kraft lignin undergoes produces the subsequent swelling and agglomeration problems which nevertheless do not seem to affect negatively the development of porosity according to the results obtained. On the other hand, the activated carbons

exhibited reasonably good mechanical properties, showing quite acceptable bulk density values in spite of their high porosity. For instance, at a 2.3 impregnation ratio and 500 °C, where the highest BET surface area (≈1800 m^2/g) and total pore volume (≈1.8 cm^3/g) were obtained, the activated carbon yielded a bulk density of 0.42 g/cm^3 as determined with mercury at 4 atm.

The swelling and agglomeration problems have to be considered if the design of a potential manufacturing process is accomplished. One way to avoid the plastic phase consists in using as the starting material kraft lignin with an ash content higher than the thoroughly washed kraft lignin used in this work (Rodríguez et al., 1989). We have observed that $ZnCl_2$-impregnated kraft lignin does not undergo the plastic phase if lignin with ash contents above 4% is used. Nevertheless, as the occurrence of the plastic phase may have an important influence on the distribution of $ZnCl_2$, this could affect the development of porosity. Work is now being carried out on this topic, but our results up to the present show that no significant differences are observed in the porous structure of the activated carbons when starting from kraft lignin with an ash content even as high as 12% (Gonzalez-Serrano, 1996).

At comparable BET surface area values these activated carbons present a porous structure fairly different to that of the ones obtained by the authors from kraft lignin through "physical" activation with CO_2 (Rodríguez-Mirasol et al., 1993a,b). When comparing activated carbons with a high BET surface area (≈1800 m^2/g), one can conclude that $ZnCl_2$ activation develops a substantially higher microporosity and a fairly lower mesoporosity. Whereas for the CO_2-activated carbons external or non-microporous surface areas higher than 450 m^2/g were reached, $ZnCl_2$-activation led to substantially lower values (≈200 m^2/g at the most).

On the other hand, a relevant difference between chemical and physical activation arises from the fact that the yield values (activated carbon/raw material) are substantially higher for the former. Thus, the aforementioned 1800 m^2/g of BET surface area can be reached through $ZnCl_2$ activation at about 40% yield whereas in the case of CO_2 activation the corresponding yield drops to 10%.

Acknowledgment

The authors acknowledge the Spanish DGICYT for financial support through the research project PB90-0004. E.G.-S. expresses her gratitude to that institution for a research grant.

Literature Cited

Barret, E. P.; Joyner, L. G.; Halenda, P. H. The determination of pore volume and area distribution in porous substances. I. Computation from nitrogen isotherms. *J. Am. Chem. Soc.* **1951**, *73*, 373.

Blasco, J. M.; Gomez-Martín, J. P.; Rodríguez-Mirasol, J.; Delgado, F.; Rodríguez, J. J. Activated carbons from olm oak wood by chemical activation. *An. Quim.* **1989**, *85*, 406.

Brunauer, S.; Deming, L. S.; Deming, W. S.; Teller, E. A theory of the van der Waals adsorption of gases. *J. Am. Chem. Soc.* **1940**, *62*, 1723.

Carrott, P. J. M.; Sing, K. S. W. In *Characterization of Porous Solids*; Unger, K. K., Rouquerol, J., Sing, K. S. W., Kral, H., Eds.; Elsevier Sci. Pub. B. V.: Amsterdam, 1988.

Carrott, P. J. M.; Roberts, R. A.; Sing, K. S. W. Standard nitrogen adsorption data for nonporous carbons. *Carbon* **1987a**, *25*, 769.

Carrott, P. J. M.; Roberts, R. A.; Sing, K. S. W. Adsorption of nitrogen by porous and non-porous carbons. *Carbon* **1987b**, *25*, 59.

Caturla, F.; Molina-Sabio, M.; Rodríguez-Reinoso, F. Preparation of activated carbon by chemical activation with $ZnCl_2$. *Carbon* **1991**, 29, 999.

Dubinin, M. M. In *Chemistry and physics of Carbon*; Walker, P. L., Jr., Ed.; Marcel Dekker: New Yorl, 1966; Vol. 2.

Gonzalez-Serrano, E. $ZnCl_2$-Chemical activation of kraft lignin. Ph.D Dissertation, University of Málaga, Málaga, Spain, 1996.

Greg, S. J.; Sing, K. S. W. *Adsorption, Surface Area and Porosity*; Academic Press: London, 1982.

Mikhail, R. H.; Brunauer, S.; Bodor, E. E. Investigation of a complete pore structure analysis. I. Analysis of micropores. *J. Colloid Interface Sci.* **1968**, *26*, 45.

Rodríguez, J. J.; Cordero, T.; Rodríguez-Mirasol, J.; Simón, A.; Bataller, A. In *Pyrolysis and gasification*; Ferrero, G. L., Maniatis, K., Buekens, A.; Bridgwater, A. V., Eds.; Elsevier Applied Science: London, 1989.

Rodríguez-Mirasol, J.; Cordero, T.; Rodríguez, J. J. Preparation and characterization of activated carbons from eucalyptus kraft lignin. *Carbon* **1993a**, *31*, 87.

Rodríguez-Mirasol, J.; Cordero, T.; Rodríguez, J. J. Activated carbons from CO_2 partial gasification of eucalyptus kraft lignin. *Energy Fuels* **1993b**, *7*, 133.

Rodríguez-Mirasol, J.; Cordero, T.; Rodríguez, J. J. CO_2-Reactivity of eucalyptus wood chars. *Carbon* **1993c**, *31*, 53.

Rodríguez-Reinoso, F. In *Carbon and Coal Gasification*; Figueiredo, J. L., Moulijn, J. A., Eds.; Martinus Nijhoff Publishers: Dordrecht, The Netherlands, 1986.

Rodríguez-Reinoso, F.; Molina-Sabio, M. Activated carbons from lignocellulosic materials by chemical and/or physical activation: an overview. *Carbon* **1992**, *30*, 1111.

Rodríguez-Reinoso, F.; Garrido, J.; Martín-Martínez, J. M.; Molina-Sabio, M.; Torregrosa, R. The combined use of different approaches in the characterization of microporous carbons. *Carbon* **1989**, *27*, 23.

Ruiz-Beviá, F.; Prats-Rico, D.; Marcilla-Gomis, A. Activated carbon from almond shells. Chemical activation 1. Activating reagent selection and variables influence. *Ind. Eng. Chem. Prod. Res. Dev.* **1984a**, *23*, 266.

Ruiz-Beviá, F.; Prats-Rico, D.; Marcilla-Gomis, A. Activated carbon from almond shells. Chemical activation 2. $ZnCl_2$ activation temperature influence. *Ind. Eng. Chem. Prod. Res. Dev.* **1984b**, *23*, 269.

Sing, K. S. W. In *Surface Area Determination;* Everet, D. H., Ottewill, R. H., Eds.; Butterworths: London. 1970.

Sing, K. S. W.; et al. Reporting Physisorption data for Gas/Solid systems with special reference to the determination of surface area and porosity. *Pure Appl. Chem.* **1985**, *57*, 603.

Torregrosa, R.; Martín-Martínez, J. M. Activation of lignocelulosic materials: a comparison between chemical, physical and combined activation in terms of porous texture. *Fuel* **1991**, *70*, 1173.

Received for review April 8, 1997
Revised manuscript received August 1, 1997
Accepted August 5, 1997[⊗]

IE970261Q

[⊗] Abstract published in *Advance ACS Abstracts,* October 1, 1997.